Applications of remote sensing techniques to managing rock slope instability risk

D. Jean Hutchinson
Department of Geological Sciences and Geological Engineering, Queen's University, Kingston, Ontario, Canada
Matthew Lato and Dave Gauthier
BGC Engineering Inc., Ottawa and Kingston, Ontario, Canada
Ryan Kromer, Matthew Ondercin, Megan van Veen and Rob Harrap
Department of Geological Sciences and Geological Engineering, Queen's University, Kingston, Ontario, Canada

ABSTRACT
The recent development of rapid, accurate and sophisticated remote sensing tools has provided valuable rock slope change data, previously impossible to obtain. The analysis techniques discussed in this paper utilize detailed and accurate models of three-dimensional geometry developed from photographs and LiDAR point clouds. Models of the rock slope from data collected at similar times can be combined, taking advantage of data at different resolutions and collected from different vantage points and platforms. Such models can be used for remote mapping of discontinuities and lithology as has been demonstrated by others. The added value for slope stability management discussed in this paper is realized when geometrical data sets from different times are compared. Depending upon the frequency of measurements and the rate of change of the rock slope, prior to slope failure it is possible to hypothesize the slope failure mode, the potential volume of the impending failure and in some cases, to provide an accurate estimate of the time of failure. In back analysis, it is possible to determine the distribution of the source zone(s), to assess the path of movement, and to calculate the volume of the source volume and accumulated debris. The case histories presented in this paper demonstrate our enhanced ability to detect and manage the risk of rock slope failure.

RÉSUMÉ
Le développement récent d'outils de télédétection rapides, précis et sophistiqués, a fourni des données précieuses sur les changements de pentes dans le roc, lesquelles étaient auparavant impossibles à obtenir. Les techniques d'analyses discutées lors de cette conférence utilisent des modèles détaillés et précis de la géométrie en 3 dimensions, développés à partir de photographies et de données Lidar. Les modèles des pentes rocheuses provenant de données prises à des moments similaires peuvent être combinés afin de mettre à profit des données de différentes résolutions et recueillies selon différents points de vue et plates-formes. De tels modèles peuvent être utilisés pour la cartographie à distance des discontinuités et des lithologies, tel que démontré par d'autres. Tel que discuté dans cette conférence, la valeur ajoutée pour la gestion de la stabilité des pentes est obtenue lorsque les modèles géométriques pris à différents moments sont comparés. En fonction de la fréquence de mesures et du taux de changement des pentes rocheuses avant la rupture de la pente, il est possible de poser l'hypothèse du mode de rupture de la pente, du volume potentiel de la rupture imminente et dans certains cas, de fournir une estimation précise du moment de la rupture. Dans l'analyse à rebours, il est possible de déterminer la distribution de la ou des zone(s) source(s), d'évaluer la trajectoire et de calculer le volume de la source et des débris accumulés. Les cas historiques présentés démontrent notre habileté à détecter et gérer les risques de rupture dans les pentes rocheuses.

1 INTRODUCTION

Remote sensing techniques, which record the geometry of the slope surface, have been successfully applied to analysis of rock slope stability for a number of years. Remote sensing techniques applied to rock slopes include photogrammetry, LiDAR and InSAR techniques as discussed by many authors (Lato et al., 2009; Sturzenegger and Stead, 2009; Abellan et al. 2014; Stock et al., 2012; Bozzano et al., 2011). In recent years, this work has been revolutionized by the development of the structure from motion analysis of photographs (Vasuki et al., 2013; Walter et al., 2009; Westoby et al., 2012) and advances in portable InSAR, radar and LiDAR scanning equipment (Figure 1), which has become cheaper, lighter and therefore easier to deploy, faster, with longer range, and more accurate.

Survey design must consider the vantage points from which the data will be acquired. Objects in front of the slope, including vegetation, rock support systems and any other infrastructure will cause sections of the slope to be obscured from the data set collected. Sections of complex slopes will be obscured by protruding parts of the slope. The position of the sensor must be considered carefully so as to optimize the data collected. Lighting conditions must be considered when acquiring photographs, both from the perspective of changing lighting conditions during the data acquisition and considering that 3-D data cannot be extracted from sections of the photo which are in deep shadow.

For complex and large objects, a more complete three- dimensional model may be generated by merging three- dimensional data sets taken from different vantage points (Lato et al., 2014).

Working with three-dimensional geometric models of rock slopes, derived from these techniques, permits the assessor to map discontinuities, collecting information about discontinuity orientation, persistence and spacing (Sturzenegger and Stead, 2009; Abellan et al., 2014). In some cases where the geometrical data is of very high resolution, joint aperture and roughness information may also be collected. With the rapid advances in equipment noted above, it is only a matter of time before it is possible that data currently collected by conventional face mapping can be mapped using software, interpreting remotely sensed data. In this case, the absolute position of the slope in mapping coordinates is not required, as the measurements are relative to the slope face, and are not required to be highly precise.

High resolution, panoramic photographs of the rock slope, taken using a DSLR camera mounted on a Gigapan tripod head, permit detailed observations of the rock slope to be made from a computer screen. This may include the presence of vegetation and seepage zones, as well as the location and condition of freshly exposed surfaces after slope failure has occurred.

The greatest value of a precise, repeatable 3-D geometry model, for rock slope assessment, is the ability to compare multi-temporal scans to detect change. This can be done using photogrammetry or LiDAR data or a combination of both techniques – the accuracy of the model surface can be in the range of cms and mms respectively (Lato et al, 2015), depending upon the design of the survey and the treatment of the data. Comparison of multi-temporal photographs is facilitated by the inclusion of survey targets with known positions in the scenes, to permit more accurate reconstruction of the three dimensional geometry. However, in circumstances where existing targets are not present and where deployment of targets is not physically practical, and for LiDAR data sets, the models are aligned to one another by matching data points found in both models that have not undergone spatial change over the time interval between the data acquisitions.

The ability to interpret this data with confidence in the accuracy of the change detected has been advancing rapidly, taking advantage of the increasingly dense data sets in both temporal and spatial domains. Collecting point cloud data continuously allows the removal of systematic errors through calibration, and random errors through averaging. Combined with spatial averaging approaches (Abellan et al. 2009) and multi-scale 3D distance calculations (Lague et al. 2013), it is now possible to detect sub mm deformation using terrestrial LiDAR in three dimensions (Kromer et al. 2015).

The ability to interpret this data with confidence in the accuracy of the change detected has been advancing rapidly, taking advantage of the increasingly dense data sets in both temporal and spatial domains. Collecting point cloud data continuously allows the removal of systematic errors through calibration, and random errors through averaging. Combined with spatial averaging approaches (Abellan et al. 2009) and multi-scale 3D distance calculations (Lague et al. 2013), it is now possible to detect sub mm deformation using a terrestrial laser scanner in 3-D (Kromer et al. 2015).

Figure 1: TLS setup in the White Canyon, approximately 350 m from the railway track.

The ability to interpret this data with confidence in the accuracy of the change detected has been advancing rapidly, taking advantage of the increasingly dense data sets in both temporal and spatial domains. Collecting point cloud data continuously allows the removal of systematic errors through calibration, and random errors through averaging. Combined with spatial averaging approaches (Abellan et al. 2009) and multi-scale 3D distance calculations (Lague et al. 2013), it is now possible to detect sub mm deformation using a terrestrial laser scanner in three dimensions (Kromer et al. 2015).

The specific slope cases presented in this report have been studied during the course of the Canadian Railway Ground Hazard Research Program, supported by CN Rail, CP, Transport Canada and the Geological Survey of Canada. These cases have all been reported on elsewhere, as referenced in this paper. As enhanced data filtering techniques have been developed, based on 2-D filter (Abellan et al., 2009) and 3-D block tracking techniques (Oppikofer et al., 2009), our ability to confidently detect smaller scale changes has increased.

As case histories are developed showing details of the change on each slope, a more detailed understanding of the failure progression and mechanism can be developed as long as the data has been collected frequently enough to detect step-wise slope changes.

2 CHANGE DETECTION

The basis of the following discussion is the ability to accurately detect changes between multi-temporal slope geometry data sets. The change detected may be the result of any number of slope processes, including deformation of a portion of the rockmass which is still in place on the slope, loss of failed blocks of rock, and accumulation of debris at the base of the slope. In some cases, it may be possible to detect change at the points where the falling rocks have impacted the slope, removing or depositing small amounts of material. An example of slope change detection mapping is illustrated in Figure 2

which is based on two LiDAR scans collected nine months apart at Mile 94.2 in the White Canyon.

It should be noted that vegetated sections of the slope may be difficult to assess as the wood and leaves will obscure the LiDAR line of sight to the rock slope beyond. In addition, change due to growth or wind induced movement for example, will affect change detection by creating spurious apparent deformation between two data sets.

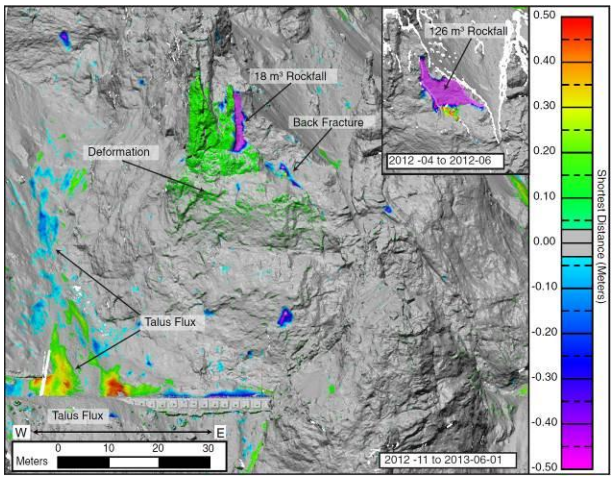

Figure 2: The shortest distance change results from November 15th, 2012 to June 1st, 2013 at Mile 94.2 in the White Canyon. Upper inset: Change results from April to June 2012. A positive difference represents deformation /displacement or gain of material and negative change represents loss of material (from Kromer et al., 2015).

2.1 Deformation Analysis leading to prediction of failure

The example demonstrating the effective prediction of the location of an impending failure, based on deformation detected from analysis of sequential LiDAR scan data analysis, is from CN Rail Ashcroft Sub, Mile 109.43. Attention was focussed on the site by a rock slope failure in November, 2012, which destroyed the existing 21 m long rock shed, deposited 53,000 m^3 of rock onto and over the tracks, and caused a 4 day outage of the track (Sturzenegger et al, 2014). This failure was anticipated by CN Rail, due to observations of failure of multiple smaller blocks from the slope and the tracks were closed prior to the rock slide event. A new rock shed was designed and installed at the site, completed in 2014, as discussed by Keegan et al (2014) and Busslinger et al (2014).

Starting in the immediate post failure period, and continuing to the present time, a series of LiDAR scans have been taken of the slope rockmass. Analysis of the LiDAR data indicated that discrete areas of the slope were moving, and analysis of the expected bounding structural features provided an estimate of the expected volume of failure from three distinct sites on the slope surface. The failure kinematics were also assessed using 3-D block tracking, which gave the orientation of displacement vectors of block movement. Slope deformation occurred at some time during the winter of 2014, stabilized during the summer of 2014, and began again in the fall, 2014. The TLS derived model of the slope prior to the failure is shown in Figure 3 (upper). Warning of these potential failures was provided, and failure occurred in December 2014 after a rain event.

The post-failure, 3-D condition of the slope was captured using oblique aerial photogrammetry (OAP; See Gauthier et al 2014, 2015; Lato et al, 2015). Approximately 500 oblique photographs were captured manually, using a digital SLR camera, from a moving helicopter. The 'structure-from-motion' approach of the commercial software 'Photoscan' (V1.1) was used to generate a detailed 3-D slope model, as shown in Figure xxx lower, which was then aligned and compared to a pre-failure TLS model. The OAP approach was deployed quickly, and the failure extent and volume were available within 72 hours of the failure, and less than 24 hours after the photos were captured.

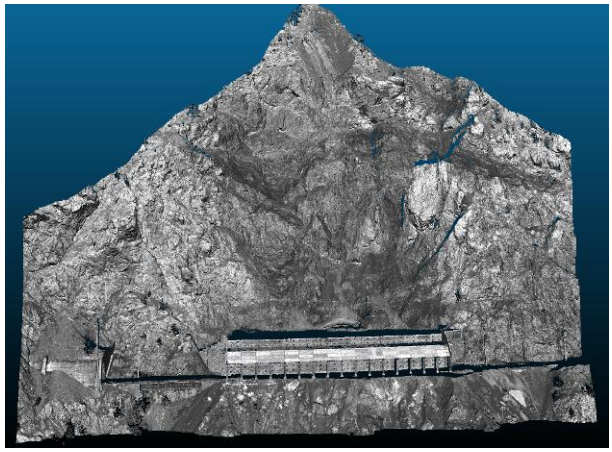

Upper

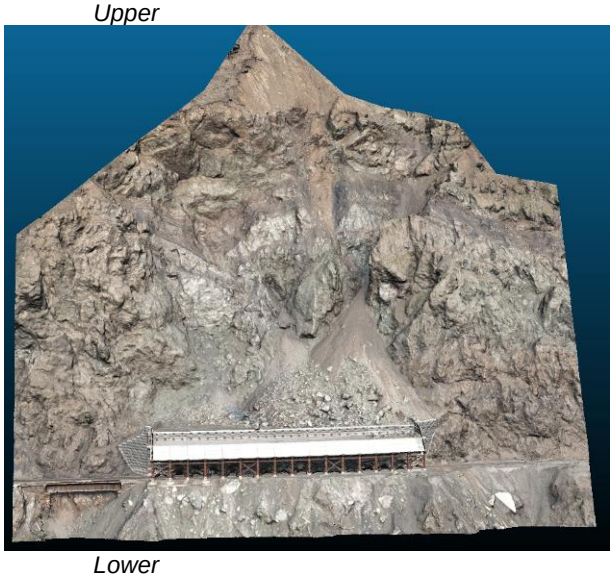

Lower

Figure 3: upper) Terrestrial LiDAR Scan of Mile 109.43, prior to failure; lower) Oblique helicopter photogrammetry, post failure in December, 2014.

Comparison between the slope geometry prior to and after the failure (Figure 4) showed that 4200 m^3 failed from the slope; a volume that was within 87.5% of the original prediction. Further information regarding this event is provided by Kromer et al (this conference).

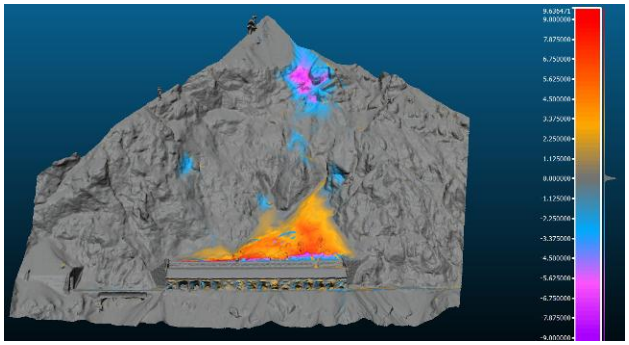

Figure 4: Change detected after rock slide events at Mile 109.43 in December, 2014. The change shown directly above the rock shed is spurious, because this section of the TLS model contained no data due to the position of the scanning vantage point from across the valley.

2.2 Failure Back Analysis

In June, 2013, a 2600 m^3 rock slope failure occurred at Mile 94.2 in the White Canyon, as shown in Figure 2, causing the track to be closed for less than 1 day for cleanup and maintenance. This area had been scanned using the LiDAR equipment multiple times in the 1.5 years before the failure occurred, and this area of the White Canyon slope was being scanned on an almost daily basis at that time to assess the frequency of data required to assess the behaviour of talus slopes. By coincidence, the area of the rock slope failure was included in most of these scans, providing a wealth of geometric data for the site.

Upon Kromer et al. (2015) application of the data processing techniques required to assess the specific slope deformation, it became apparent that deformation involving rotation and tilt was occurring prior to the failure, subsequently interpreted to be the result of opening of the back scarp fracture. In addition, it was observed that small volume blocks were moving and detaching from the rockmass around the perimeter of the eventual larger volume block failure (Figure 6). It is possible to track the velocity of movement of individual points on an object, from sequential data sets, as shown in Figure 7. This permits an evaluation of the rate of deformation and may form the basis for time to failure assessment in future cases.

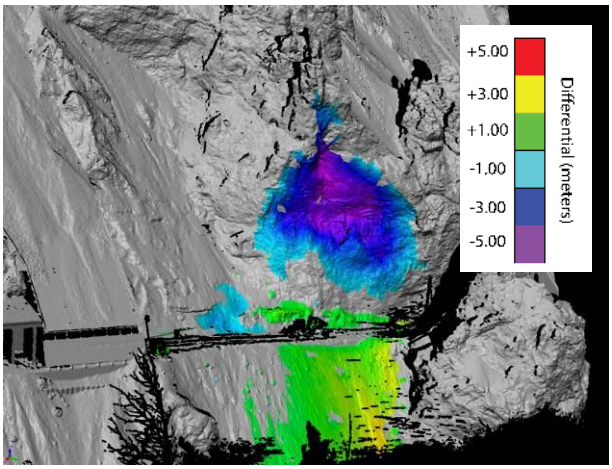

Figure 5: June, 2012, rock slope failure in the White Canyon. Change detection based on LiDAR data collected one day prior to the failure and during track clear up. The shadow of the excavator working to clear the tracks can be seen in the image.

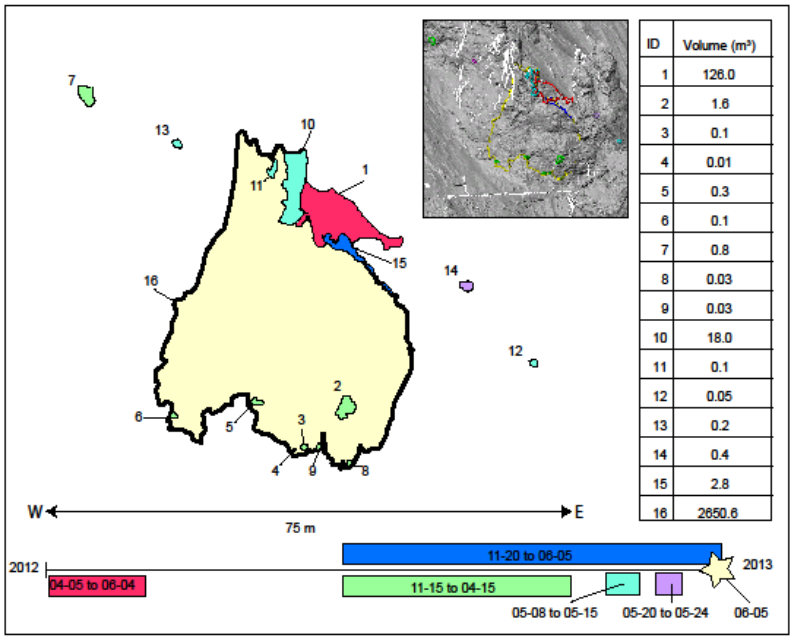

ID	Volume (m^3)
1	126.0
2	1.6
3	0.1
4	0.01
5	0.3
6	0.1
7	0.8
8	0.03
9	0.03
10	18.0
11	0.1
12	0.05
13	0.2
14	0.4
15	2.8
16	2650.6

Figure 6: Rockfall events detected prior to 2600 m^3 failure at Mile 94.2. Event ID numbers are sequential through time.

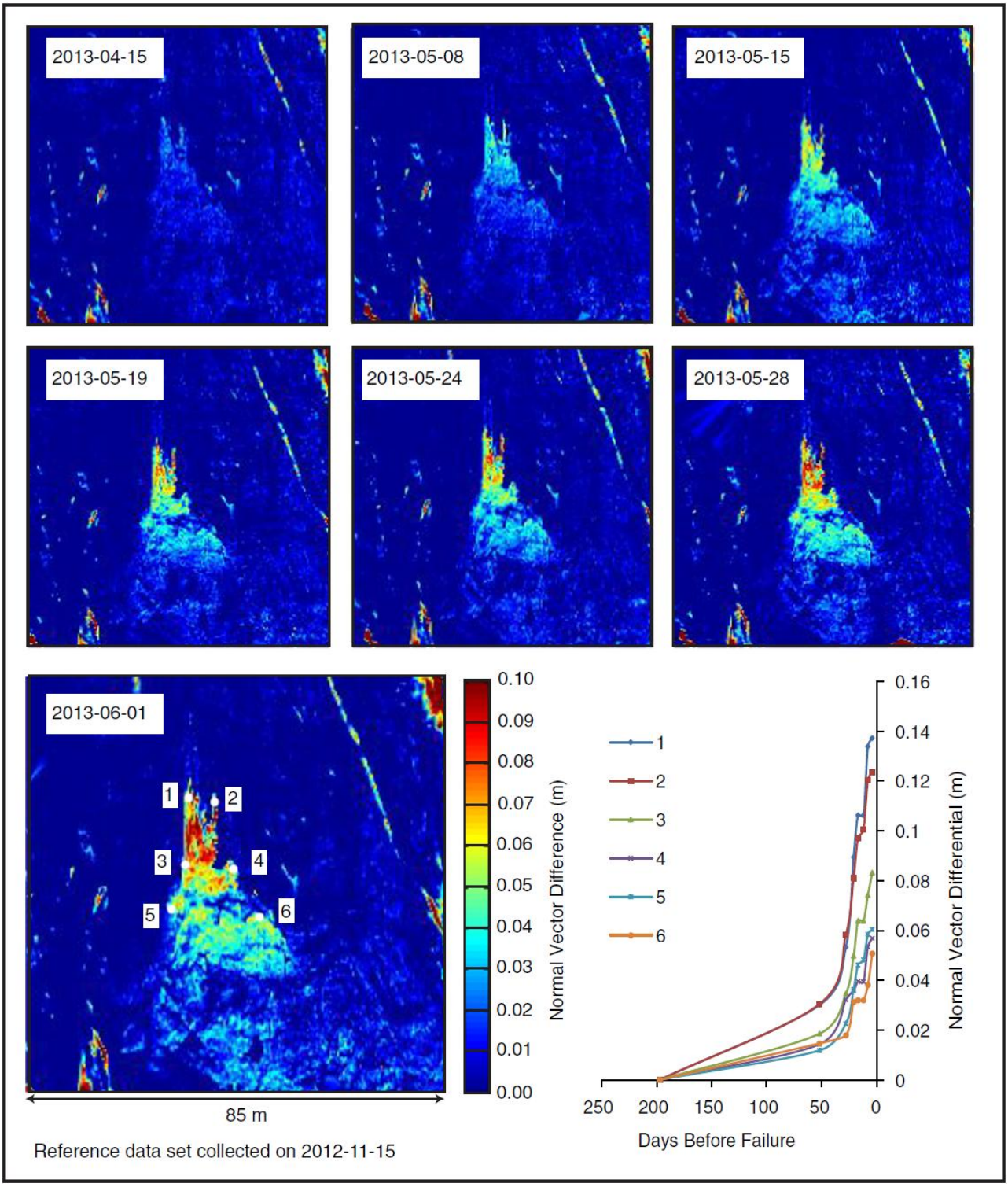

Figure 3: Filtered normal vector differences based on a reference data set collected on 2012-11-20 as compared to each successive scan for Mile 94.2 in the White Canyon, until just prior to the 2600 m^3 failure. Bottom right graph of quantitative assessment of differences for points 1 to 6 (from Kromer et al. 2015) shows the larger movements of the top of the block relative to the bottom, and along the left versus the right side of the block.

3 ROCK FALL DATA COLLECTION

An understanding of the nature of rockfall hazards is an important component of risk assessment, supporting track management in hazardous areas.

3.1 Detailed case histories for model calibration

The collection of frequent LiDAR data, at high resolution, permits detection of cases to be used for rockfall model validation (Ondercin et al, 2014). When a scan is collected soon after a rockfall, it may be possible to observe impact points along the slope, which are interpreted to be located along the path of the rockfall. An example of this can be seen in Figure 4, where areas of loss along ledges in the slope are interpreted to be the result of impacts during the rockfall event. Furthermore, the end locations of nearly all of the material involved in the rockfall event can be determined, even if the rock fragments have become distributed across the slope during the failure event. While parameters such as the pass height of the rockfall and the velocities of the rockfalls cannot be determined from this change detection, the path and stopping point of the rocks can be used as input for rockfall model verification.

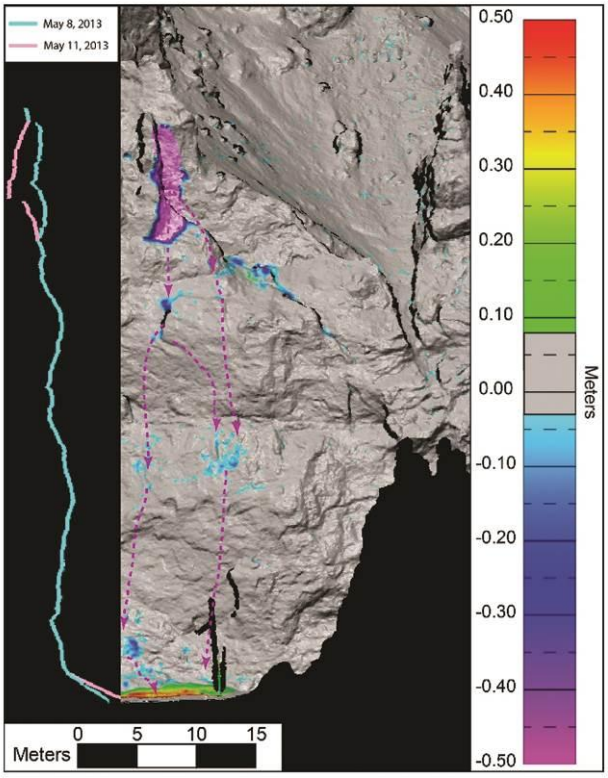

Figure 4: LiDAR change detection and probable paths of rockfall (from Ondercin et al. 2014)

3.2 Development of case history database

One important input to risk assessment is the frequency-magnitude relationship of rockfall events, which can be evaluated through the use of a rockfall database. While traditional rockfall inventories may contain estimates of event volumes, event dates, track mileage, and possible source zones or triggering mechanisms, these inventories are often incomplete and may be subject to errors and incomplete data collection. Rockfall source zones can be difficult to identify in the field, especially on large complex slopes. A drawback of using traditional rockfall inventories for frequency-magnitude analysis is the incomplete sampling of small rockfall events (Hungr et al., 1999).

In the White Canyon area, slide detector fences provide warning of rockfall events that traverse the track area; however, these reports only contain information on the time and location of the event, and are lacking volume estimates and information about source zone locations and characteristics.

A database has been created in order to gain an understanding of the spatial and temporal distribution of rockfall events and their failure mechanisms. Small volume rockfall events are included within the data collected, that would not generally be reported on the basis of visual inspections. Once rockfalls are located and volumes are calculated using LiDAR change detection, the gigapan images can be used to gain additional qualitative information about the rockfall events. LiDAR data collected over the past three years is currently being used to populate this database and once sufficient information is collected, the frequency-magnitude data as well as information on the spatial distribution of rockfalls will be evaluated for use in risk management analyses.

A preliminary case study was completed to compare data obtained between November 2014 and February 2015 in the White Canyon, the details of which are discussed by van Veen et al., (2015). During this time period, 387 rockfalls were initiated from rock outcrops on the slope, as identified from LiDAR change detection analysis. The point of deposition of these rocks is not known, due to the number of different events cumulatively affecting the slope over the 4 months of elapsed time between data acquisitions. Slide detector fence (SDF) data for the corresponding time period shows 46 activations requiring repair to and reactivation of the warning system. At this time, the volume of rock required to damage the SDF enough to require repair is unknown, but it is assumed that smaller volume fall events would pass through the wires without triggering an activation. Activations could be the result of one or more rocks falling to track level, in one or more locations along the canyon. This could also be the result of ice-fall in these winter months.

Analysis of these LiDAR datasets provided insight into the spatial distribution of rockfalls of varying magnitude, as shown in Figure 5. With further analysis, it may be possible to discern patterns of precursor deformation and spatially significant patterns of smaller scale rockfalls providing early warning of impending larger scale failure events, particularly when additional information about rockfall events in the canyon is known. At this site, this information may be available from data collected from a prototype microseismic monitoring system and from rockfall information collected by track supervisors and maintenance personnel.

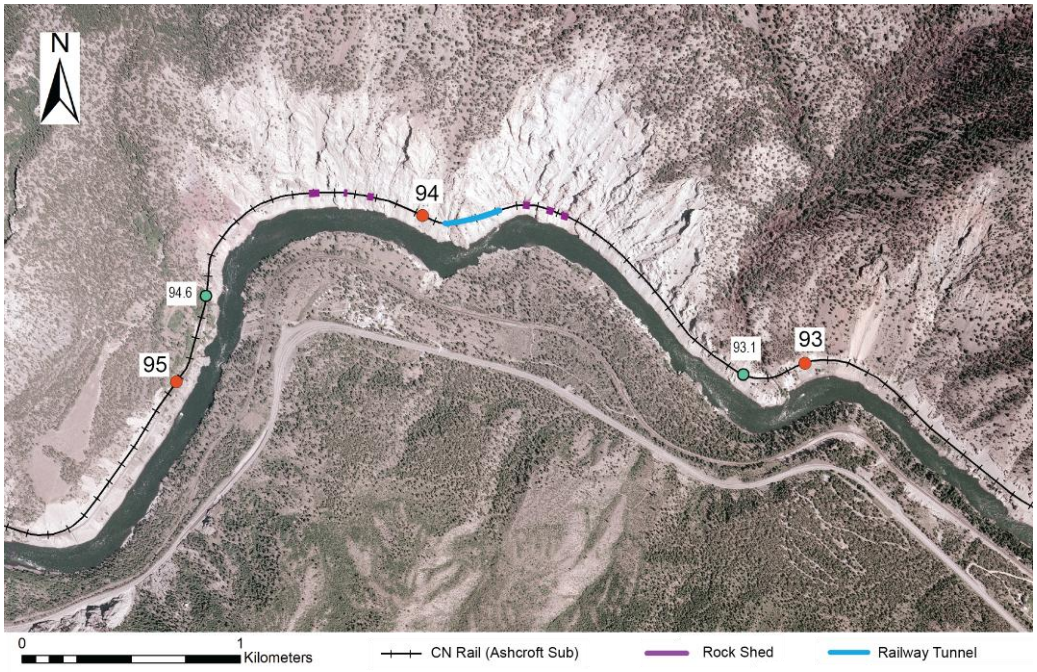

Figure 5: The White Canyon corridor extends from Mile 93.1 to Mile 94.6 on CN's Ashcroft sub. The location of the tunnel dividing the West and East portions of the slope, as well as the six rock sheds is shown.

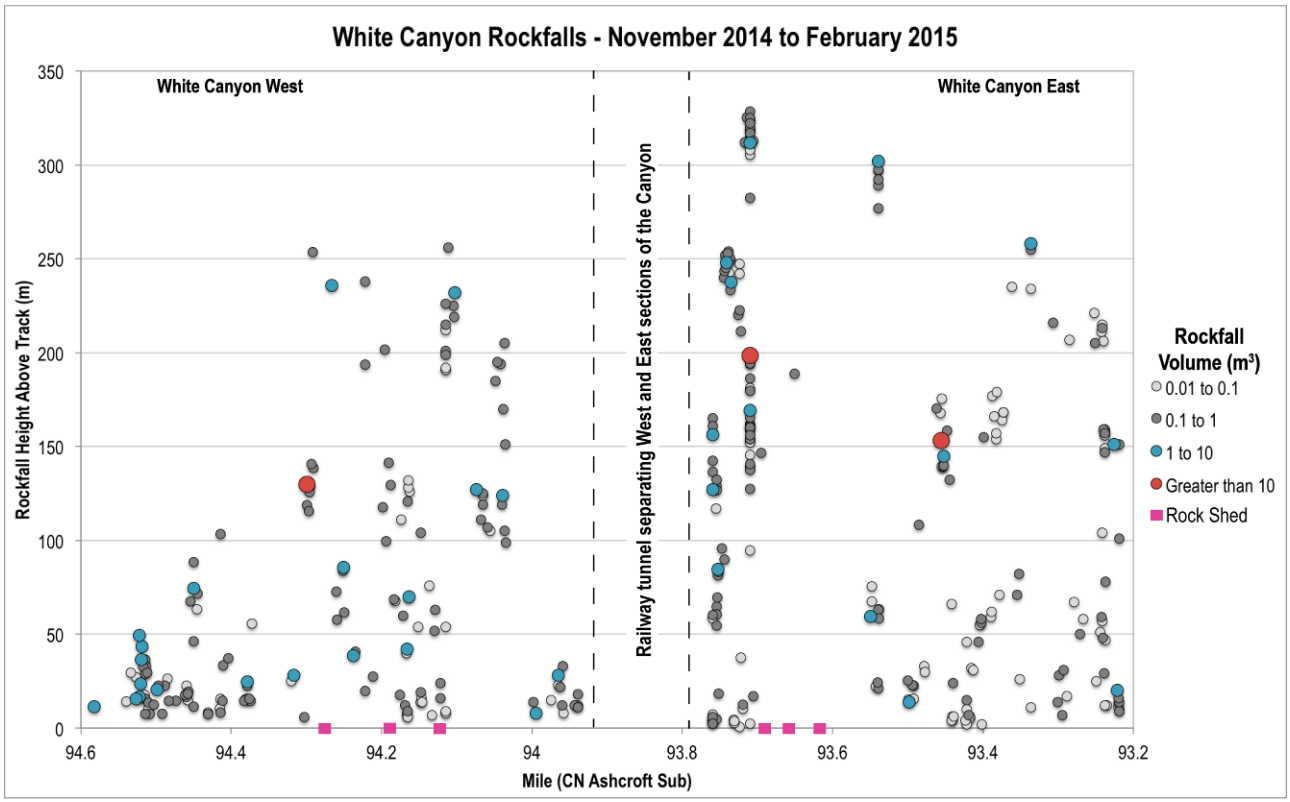

Figure 6. Distribution of rockfall source zones by mile, as determined from LiDAR change detection analysis comparing data sets taken in November 2014 and February 2015. Only the events recorded as initiating from rock outcrop are included in this figure. Movement in talus channels is ongoing, but is not recorded here.

4 SELECTION OF APPROPRIATE REMOTE SENSING APPROACHES

The application of remote sensing approaches to rock slope stability assessment are affected by the frequency of measurement, the orientation of the scans and their spatial overlap, and range, accuracy and precision of the instrument used, and any adverse atmospheric conditions including smoke, fog and rain, for example. As noted previously, the data collection techniques utilized in this work include LiDAR and photogrammetry. These techniques can be deployed from several platforms using equipment which supplies data at different resolutions, as shown in Figure 7. The optimal selection of scan orientation, platform and equipment is discussed by Lato et al (2015), with a summary provided in Table 1.

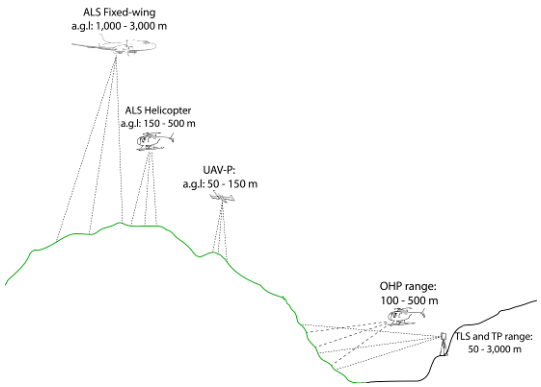

Figure7: 3D remote data collection platforms used for rock slope mapping and monitoring (from Lato et al., 2015)

Table 1: Data resolution required for common 3-D data analysis tasks and the associated technologies suitable for data collection.

	Resolution (pts/m^2)	TLS	TP	OHP	ALS	UAV-P
Map regional faults and land formations	5				✔	
Map fractures with length >10 m (tree coverage)	10				✔	
Map fractures with length >5 m (tree coverage)	20				✔	
Map fractures with length >5 m	20	✔	✔	✔	✔	✔
Map fractures with length >1 m	100	✔	✔	✔		✔
Map fractures with length >0.5 m	500	✔	✔	✔		✔
Map fractures with length >0.1 m	1000	✔	✔	*		*
Map slope change > 1m^3 (tree coverage)	20				✔	
Map slope change > 1 m^3	20	✔	✔	*	✔	✔
Map slope change > 0.25 m^3	100	✔	✔	*		*
Map slope change > 0.1 m^3	500	✔	✔	*		*
Map line of sight visibility	20				✔	

* OHP and UAV-P are emerging technologies with presently unknown capabilities. Preliminary research indicates that both technologies could be used to map rockfall slope activity in the range of 0.25 m^3 and smaller, but there are no published results to corroborate this.

The frequency of data collection campaigns depends on the expected deformation mechanism and interpretation of the failure mode. Optimal data collection will provide a baseline set of data before slope deformation has begun, but before the deformation rate accelerates or smaller scale pre-cursor failure events start to happen. Early recognition of potential impending failure provides the opportunity for early warning to be provided, monitoring to be enhanced, and potential mitigation solutions to be considered and implemented.

Overall rock slope hazard and risk may be assessed in a number of ways, including using hazard rating schemes based on qualitative approaches (subjective expert opinion), semi-quantitative approaches (weighted factors considering slope geometry and geotechnical factors, calculated following a hazard rating system, or within a GIS system utilizing susceptibility mapping techniques) and/or quantitative approaches (calculated probability and consequence of failure based on probabilistic modelling of the slope failure condition). Change detection approaches serve to focus attention on the sites of greatest potential hazard, assuming that impending failure is preceded by slope deformation and change, permitting the assessment of failure volume, location, mechanism and possibly a prediction of time until failure is expected.

5 FUTURE WORK

Work is ongoing on this project, with regular field work to repeat scans and photographs of the rock slopes, and the addition of aerial LiDAR scanning. As data is collected, we hope to better define the logic of the spatial and temporal relationship between pre-cursor event, to enhance early warning before failure occurs.

Work will also continue to define optimal survey design considering complex slope geometry and access limitations and to process the data to extract additional detail. Scan location and frequency should relate to the deformation patterns observed, and the expected failure mode.

ACKNOWLEDGEMENTS

The writers would like to acknowledge the contribution of a number of individuals to the paper. Much of this work has been conducted for the Canadian Railway Ground Hazards Research Program. Support by NSERC, CN Rail, and Canadian Pacific is greatly appreciated.

REFERENCES

Abellán, A., Jaboyedoff, M., Oppikofer, T., Vilaplana, J.M., 2009. Detection of millimetric deformation using a terrestrial laser scanner: experiment and application to a rockfall event. *Nat.Hazards Earth Syst. Sci.*, 9, 365–372. http://dx.doi.org/10.5194/nhess-9-365-2009.

Abellán, A., Oppikofer, T., Jaboyedoff, M., Rosser, N.J., Lim, M., and Lato, M.J. 2014. Terrestrial laser scanning of rock slope instabilities. *Earth Surface Processes and Landforms,* 39, 80-97.

Bozzano, F., Cipriani, I., Mazzanti, P., Prestininzi, A. 2011. Displacement patterns of a landslide affected by human activities: insights from ground-based InSAR monitoring. *Nat. Hazards*, 59, 1377–1396. http://dx.doi.org/10.1007/s11069-011-9840-6.

Busslinger, M., O. Hungr, T. Keegan, W. Wu, T. Edwards. 2014. Rock Mass Fall – Rock Avalanche Design Loads for Railway Track Protection Structures, in *Geohazards 6: 6th Canadian Geohazards Conference*, Kingston, ON, June 15-18.

Dewez, T., Rohmer, J., Regard, V., 2013. Probabilistic coastal cliff collapse hazard from repeated terrestrial laser surveys: case study from Mesnil Val (Normandy, northern France). *J. Coast. Res.*, 65, 702–707. http://dx.doi.org/10.2112/SI65-119.1.

Gigli, G., Frodella, W., Garfagnoli, F., Morelli, S., Mugnai, F., Menna, F., and Casagli, N. 2013. 3-D geomechanical rock mass characterization for the evaluation of rockslide susceptibility scenarios. *Landslides*, 11, 131–140. doi:10. 1007/s10346-013-0424-2.

Hungr, O., Evans, S. and Hazzard, J. 1999. Magnitude and frequency of rock falls and rock slides along the main transportation corridors of Southwestern British Columbia, *Canadian Geotechnical Journal*, 36(2): 224-238.

Keegan, T., B. Willoughby, T. Edwards, M. Busslinger, M. Sturzenegger and A. Wen. 2014. Construction of a Composite Barrier Wall/Rock Shed Structure at Mile 109.43 of CNR's Ashcroft Subdivision, in *Geohazards 6: 6th Canadian Geohazards Conference*, Kingston, ON, June 15-18.

. Kromer, R. A.; Hutchinson, D. J.; Lato, M. J.; Gauthier, D.; Edwards, T. 2015. Identifying rock slope failure precursors using LiDAR for transportation corridor hazard management. Engineering Geology, 195, 93–103.

Kromer, R.A., Abellan, A., Hutchinson, D.J., Lato, M.J., Jaboyedoff, M.2015 submitted. 4D De-noising and Systematic Calibration for Multi-temporal Point Cloud Change Detection. Journal of Remote Sensing.

Lato, M., Hutchinson, J., Diederichs, M., Ball, D., Harrap, R., 2009. Engineering monitoring of rockfall hazards along transportation corridors: using mobile terrestrial LiDAR. *Nat. Hazards Earth Syst. Sci.*, 9, 935–946. http://dx.doi.org/10.5194/nhess-9-935-2009.

Lato, M. J., Gauthier, D., & Hutchinson, D.J. 2015. Selecting the Optimal 3D Remote Sensing Technology for the Mapping, Monitoring and Management of Steep Rock Slopes Along Transportation Corridors. In *Transportation Research Board 94th Annual Meeting* (No. 15-3055).

Lato, M. J., Hutchinson, D. J., Gauthier, D., Edwards, T., & Ondercin, M. 2014. Comparison of airborne laser scanning, terrestrial laser scanning, and terrestrial photogrammetry for mapping differential slope change in mountainous terrain. *Canadian Geotechnical Journal*, 52(999), 1-12.

Ondercin, M., Kromer, R., Hutchinson, D.J., and Gauthier, D. (2014). A Sensitivity analysis of 3D rockfall models calibrated using rockfall trajectories inferred from LiDAR change detection and inspection of gigapixel photographs. In: Proceedings, 6th Canadian Geohazards Conference, Kingston On, 15-18 June 2014.

Oppikofer, T., Jaboyedoff, M., Blikra, L., Derron, M.H., Metzger, R., 2009. Characterization and monitoring of the Åknes rockslide using terrestrial laser scanning. Nat. *Hazards Earth Syst. Sci.*, 9, 1003–1019. http://dx.doi.org/10.5194/nhess-9-1003-2009.

Stock, G.M., Martel, S.J., Collins, B.D., Harp, E.L., 2012. Progressive failure of sheeted rock slopes: the 2009–2010 Rhombus Wall rock falls in Yosemite Valley, California, USA. *Earth Surface Processes Landforms*. 37, 546–561. http://dx.doi.org/10.1002/esp.3192.

Sturzenegger, M., T. Keegan, A. Wen, D. Willms, D. Stead and T. Edwards. 2014. LiDAR and Discrete Fracture Network Modeling for Rockslide Characterization and Analysis, in *Engineering Geology for Society and Territory – Volume 6*, ed. G. Lollino et al. Switzerland: Springer International.

Sturzenegger,M., and Stead, D., 2009. Close-range terrestrial digital photogrammetry and terrestrial laser scanning for discontinuity characterization on rock cuts. *Engineering Geology*, 106, 163–182. http://dx.doi.org/10.1016/j.enggeo.2009.03.004.

van Veen, M. Hutchinson, D.J., Kromer, R., Lato, M., Gauthier, D., and Edwards, T. 2015. Frequency-magnitude of rockfall events for hazard analysis; a comparison of data from LiDAR scanning with traditional methods of reporting, *Canadian Geotechnical Conference*, Quebec City.

Vasuki, Y., Holden, E. J., Kovesi, P., & Micklethwaite, S. 2013. A geological structure mapping tool using photogrammetric data. *ASEG Extended Abstracts*, (1), 1-4.

Walter, M., Niethammer, U., Rothmund, S., & Joswig, M. (2009). Joint analysis of the Super-Sauze (French Alps) mudslide by nanoseismic monitoring and UAV-based remote sensing. First Break, 27(8).

Westoby, M. J., Brasington, J., Glasser, N. F., Hambrey, M. J., & Reynolds, J. M. (2012). 'Structure-from-Motion' photogrammetry: A low-cost, effective tool for geoscience applications. Geomorphology, 179, 300-314.